

Ultrafast Phenomena VI

Proceedings of the 6th International Conference,
Mt. Hiei, Kyoto, Japan, July 12–15, 1988

Editors: T. Yajima, K. Yoshihara,
C. B. Harris, and S. Shionoya

With 487 Figures

Springer-Verlag Berlin Heidelberg New York
London Paris Tokyo

Contents

Part I	Generation, Amplification and Compression of Ultrashort Light Pulses	
<hr/>		
Chirped Pulse Amplification: Present and Future By P. Maine, D. Strickland, M. Pessot, J. Squier, P. Bado, G. Mourou, and D. Harter (With 5 Figures)		2
Generation of Intense 20-fs Pulses and Their Application in Multiphoton Ionization By P.B. Corkum, C. Rolland, and S.L. Chin (With 2 Figures)		8
Generation of Tunable 9-fs Optical Pulses in the Near Infrared By P.C. Becker, H.L. Fragnito, R.L. Fork, F.A. Beisser, and C.V. Shank (With 2 Figures)		12
Amplification and Compression of 16-fs Spectrally Broadened Pulses to the Microjoule Level at 10 kHz By P. Georges, J.P. Chambaret, F. Salin, G.R. Boyer, M.A. Franco, G. Le Saux, G. Roger, and A. Brun (With 3 Figures)		15
Generation of High-Repetition-Rate 14-fs Amplified Pulses Using a Q-Switched CW YAG Pumping Laser By Y. Ishida, T. Tokizaki, and T. Yajima (With 2 Figures)		19
10 kHz-Rate Amplification of 40-fs Optical Pulses at Low Pumping Energy By E.V. Khoroshilov, I.V. Kryukov, P.G. Kryukov, and A.V. Sharkov (With 1 Figure)		22
Generation of 29-fs Pulses from a Synchronously Pumped Dye Laser and Its Cavity-Dumping Technique By M. Nakazawa, H. Kubota, and K. Kurokawa (With 4 Figures) .		24
Colliding Pulse Mode-Locked Femtosecond Laser Using Binary- Energy-Transfer Gain Dye Mixture By M. Mihailidi, Y. Budansky, X.M. Zhao, Y. Takiguchi, and R.R. Alfano (With 3 Figures)		27

Saturable Amplification Without Pulse Broadening By J.D. Kafka and J.B. Clark (With 2 Figures)	30
General Analysis of Optical Cavities for Femtosecond Dye Lasers By S. De Silvestri, Liu Yu-Pu, V. Magni, and O. Svelto (With 3 Figures)	33
Chirp-Compensation Cavity-Mirrors of Small Third-Order Dispersion for a Femtosecond Pulse Laser By M. Yamashita, S. Kaga, K. Torizuka, and T. Sato (With 1 Figure)	37
Theoretical and Experimental Study of Synchronously Pumped Dispersion Compensated Femtosecond Fiber Raman Lasers and Amplifiers By E.A. Golovchenko, E.M. Dianov, P.V. Mamyshev, A.M. Prokhorov, and D.G. Fursa (With 3 Figures)	40
Compression of the High Energy Pulsed Mode-Locked Nd:YLF and Nd:YAG Lasers By P.H. Chiu, P. Pax, and R. Aubert (With 4 Figures)	44
Active Pulse Compression By B.H. Kolner (With 1 Figure)	47
Two Novel Techniques for Femtosecond Pulse Compression: Utilization of Induced Phase Modulation and Highly Nonlinear Organic-Fibers By M. Yamashita, K. Torizuka, T. Shiota, and T. Sato (With 2 Figures)	50
Generation of Sub-100-fs Pulses at 532 nm from Modulation Instability Induced by Cross-Phase Modulation in Optical Fibers By P.L. Baldeck, R.R. Alfano, and G.P. Agrawal (With 2 Figures)	53
Femtosecond Continuum Generation in Fibers Near 1.6 μm By M.N. Islam, G. Sucha, J.P. Gordon, I. Bar-Joseph, and D.S. Chemla (With 3 Figures)	56
Picosecond Pulse Generation by Two-Photon Induced Amplified Spontaneous Emission By A. Penzkofer and P. Qiu (With 3 Figures)	61
Mode-Locked Continuous Wave Titanium Sapphire Laser By J.D. Kafka, A.J. Alfrey, and T. Baer (With 2 Figures)	64
Non-soliton Modelocking of an F-Centre Laser with a Nonlinear External Cavity By K.J. Blow, D.S. Forrester, and B.P. Nelson (With 2 Figures)	67

Significance of Enhanced Differential Gain for Short Pulse Generation in Semiconductor Lasers By T. Sogawa, Y. Arakawa, and T. Kamiya (With 3 Figures)	70
Characteristics of Picosecond Pulse Amplification by a Traveling-Wave InGaAsP Optical Amplifier By J.M. Wiesenfeld, G. Eisenstein, R.S. Tucker, G. Raybon, and P.B. Hansen (With 4 Figures)	73
A Few Tens of Picoseconds Light Source of Continuous Spectrum with Cherenkov Radiation By S. Owaki, T. Okada, Y. Kimura, S. Nakahara, and K. Sugihara (With 4 Figures)	77

Part II Generation of Short-Wavelength Ultrashort Light Pulses

Generation of High Power UV Femtosecond Pulses By S. Szatmári and F.P. Schäfer (With 5 Figures)	82
Subpicosecond UV Pulse Generation for Multiterawatt XeCl and KrF Lasers. By M. Watanabe, A. Endoh, N. Sarukura, and S. Watanabe (With 5 Figures)	87
Subpicosecond, High-Brightness Excimer Laser Systems By A.J. Taylor, R.B. Gibson, J.P. Roberts, C.S. Lester, T.R. Gosnell, S.E. Harper, and C.R. Tallman (With 2 Figures)	91
Sub-100-fs Pulse Generation from Continuously Pumped Coumarin Dye Lasers in the Green-Blue By P.M.W. French and J.R. Taylor (With 3 Figures)	94
Generation of Intense Tunable Femtosecond Pulses in the Deep Blue Spectral Region By D.K. Negus, B.C. Couillaud, and R. Brady (With 3 Figures) . .	97
New Developments in Ultraviolet and High Intensity Femtosecond Sources. By M.C. Downer, G. Focht, T.R. Zhang, W.M. Wood, D.H. Reitze, and G.W. Burdick (With 3 Figures)	101

Part III Propagation, Control and Measurement of Ultrashort Light Pulses

Dispersive Pulse Shaping and Soliton-like Pulses in a Passively Mode-Locked Dye Ring Laser. By D. Kühlke, T. Bonkhofer, U. Herpers, and D. von der Linde (With 2 Figures)	106
---	-----

Control and Characterization of Soliton-like Pulses in a Femtosecond Dye Laser By W.L. Nighan, Jr., T. Gong, and P.M. Fauchet (With 4 Figures)	109
Solitons in the Region of the Minimum Group Dispersion Wavelength of a Single Mode Optical Fibre. By A.S. Gouveia-Neto, M.E. Faldon, and J.R. Taylor (With 3 Figures)	112
Femtosecond Pulse Tailoring for Dark Soliton Propagation Studies By A.M. Weiner, J.P. Heritage, R.J. Hawkins, R.N. Thurston, E.M. Kirschner, D.E. Leaird, and W.J. Tomlinson (With 4 Figures)	115
White Light Interferometric Measurements of Femtosecond Group Delay in Optical Components with 1-fs Precision By W.H. Knox, N.M. Pearson, K.D. Li, and C.A. Hirlimann (With 5 Figures)	118
Caution! IR Pulses May Be Distorted After Propagation in Atmospheric Air By A. Seilmeier, M. Wörner, and W. Kaiser (With 2 Figures)	121
Pulse Front Distortion in Lens Systems By S. Szatmári and G. Kühnle (With 6 Figures)	124
Blue Shifting of Intense Femtosecond Pulses in Gas Breakdown and Solid State Plasmas. By M.C. Downer, G. Focht, D.H. Reitze, W.M. Wood, and T.R. Zhang (With 3 Figures)	128
Time Domain Phase Conjugation and Twin Fields of Picosecond Light Continuum By A. Jankauskas, A. Piskarskas, and A. Stabinis (With 2 Figures)	132
Picosecond to Femtosecond Optical Synthesizers By T. Kobayashi, A. Morimoto, M. Doi, Bong Young Lee, and T. Sueta (With 5 Figures)	135
Synthesis and Applications of Arbitrarily Shaped Optical Pulses in Coherent Spectroscopy and Nonlinear Pulse Propagation By M. Haner and W.S. Warren (With 2 Figures)	139
A New Method for Measuring Ultrashort Optical Pulses By K. Naganuma, K. Mogi, and H. Yamada (With 5 Figures)	142
A Phase Sensitive Single Pulse Autocorrelator for Ultrashort Laser Pulses. By G. Szabó, Z. Bor, and A. Müller (With 2 Figures)	146
Single Shot Measurement of Optical Phase Modulation with Subpicosecond Resolution by Temporal Holography By F. Reynaud, F. Salin, A. Barthélémy, A. Brun, and C. Froehly (With 3 Figures)	149

A Method of Evaluation of Ultrashort Light Pulses Based on Self-Phase Modulation By H. Yoshiyama, Y. Shio, A. Imaizumi, H. Motoyama, M. Nakajima, S. Tanaka, H. Kobayashi, A. Watanabe, and H. Saito (With 3 Figures)	153
Measurement of Femtosecond Pulsewidths Using Interference Autocorrelation By Gong Zhenglie, Huang Zhengyi, Xu Ziguang, Qian Shurong, Xiang Wanghua, and Wang Qingyue (With 4 Figures)	156
Recent Advances Towards a 100-fs-Resolution Streak Camera By A. Finch, Y. Liu, H. Niu, W. Sibbett, W.E. Sleat, D.R. Walker, Q.L. Yang, and H. Zhang (With 3 Figures)	159

Part IV Opto-Electronics and Communications

Advanced Optical Communications Technologies Utilizing Ultrashort Optical Pulses By M. Saruwatari, K. Nakagawa, S. Kawanishi, and A. Takada (With 5 Figures)	164
Femtosecond All-Optical Switching in Nonlinear Directional Couplers By A.M. Weiner, Y. Silberberg, S.R. Friberg, B.G. Sfez, and P.W. Smith (With 8 Figures)	169
Picosecond Switching of Surface-Emitting Laser Diodes By K. Kojima and K. Kyuma (With 7 Figures)	174
Ultrafast Optical Switching Based on Stimulated Emission in GaAs/AlGaAs Multiple Quantum Wells By J.L. Oudar, C. Tanguy, J.P. Chambaret, and D. Hulin (With 2 Figures)	179
Picosecond Characterization of InGaAs/InAlAs Resonant Tunneling Barrier Diode by Electro-Optic Sampling By A. Tackeuchi, T. Inata, S. Muto, and E. Miyauchi (With 3 Figures)	182
Tunneling-Time Measurements of a Resonant Tunneling Diode By J.F. Whitaker, T.B. Norris, G. Mourou, T.C.L.G. Sollner, W.D. Goodhue, X.J. Song, and L.F. Eastman (With 3 Figures) . . .	185
Electro-Optic Sampling of a Flip-Chip with a Distributed Feedback Laser Diode By K. Joshin, K. Kamite, T. Mimura, and M. Abe (With 3 Figures)	189

A New Scheme of Resolution Improved Electrooptic Sampling
 By T. Kamiya, R. Takahashi, H. Kamiyama, H.F. Liu, and I. Tanaka
 (With 1 Figure) 192

Metal-Semiconductor-Metal Photodiode on GaInAs Exhibiting Very
 Fast Response
 By O. Wada, H. Nobuhara, H. Hamaguchi, T. Mikawa,
 A. Tackeuchi, and T. Fujii (With 3 Figures) 195

Picosecond HEMT Photodetector: Improvement of Response Speed
 at Low Temperatures
 By T. Umeda, Y. Cho, H. Tanaka, and Nion Sock Chang
 (With 2 Figures) 198

Picosecond Transient Propagation Studies on Thin-Film Y-Ba-Cu-O
 Transmission Lines
 By J.M. Chwalek, D.R. Dykaar, J.F. Whitaker, T.Y. Hsiang,
 G. Mourou, D.K. Lathrop, S.E. Russek, and R.A. Buhrman
 (With 2 Figures) 201

Greater than 100 GHz Traveling Wave Modulator
 By J. Nees, S. Williamson, and G. Mourou (With 4 Figures) 205

Part V Applications to Solid-State Physics

Ultrafast Scattering and Energy Relaxation of Optically Excited
 Carriers in GaAs and AlGaAs
 By W.Z. Lin, R.W. Schoenlein, M.J. LaGasse, B. Zysset, E.P. Ippen,
 and J.G. Fujimoto (With 7 Figures) 210

Time-Resolved Terahertz Conductivity of Photoinjected Hot
 Electrons in Gallium Arsenide
 By M.C. Nuss (With 2 Figures) 215

Femtosecond Transients and Dynamic Stark Effect in
 Semiconductors
 By N. Peyghambarian, B. Fluegel, S.W. Koch, J. Sokoloff,
 M. Lindberg, M. Joffre, D. Hulin, A. Migus, and A. Antonetti
 (With 3 Figures) 218

Bleaching of an Exciton Line Using Sub- T_2 Pulses: Artifact or
 Reality?
 By M. Joffre, D. Hulin, J.P. Chambaret, A. Migus, A. Antonetti,
 and C. Benoit à la Guillaume (With 2 Figures) 223

Picosecond-Laser-Driven Shock Wave Dynamics in Semiconductors
 By X.Z. Lu, R. Garuthara, S. Lee, and R.R. Alfano (With 6 Figures) 226

Hole Burning in the Free Exciton Line in GaSe By F. Minami, A. Hasegawa, K. Azuma, and K. Inoue (With 2 Figures)	229
High Density Femtosecond Excitation of Hot Carrier Distributions in InP and InGaAs By W. Kütt, K. Seibert, and H. Kurz (With 2 Figures)	233
Single-Shot Reflectivity Study of the Picosecond Melting of Silicon Using a Streak Camera By Juen-Kai Wang, P. Saeta, M. Buijs, M. Malvezzi, and E. Mazur (With 2 Figures)	236
Subpicosecond Transient Grating Experiments in Amorphous Semiconductors By G. Noll, E. Göbel, and U. Siegner (With 2 Figures)	240
Femtosecond Dynamics of Optical Nonlinearities in Wide-Gap II–VI Semiconductors By J. Puls, W. Rudolf, F. Henneberger, D. Lap, V. Petrov, U. Stamm, and B. Wilhelmi (With 2 Figures)	243
Nonlinear Process-Induced Higher-Order Components of a Picosecond Transient Grating in CdS By H. Saito and A. Watanabe (With 3 Figures)	246
Dynamics of Exciton-Polariton Luminescence with High Repetition Tunable UV Picosecond Pulses By T. Kuga, M. Kuwata, H. Akiyama, T. Hirano, and M. Matsuoka (With 3 Figures)	249
Picosecond Dynamics of Exciton Polaritons in CuCl Single Crystals By T. Itoh, Jin Fashan, Y. Iwabuchi, and T. Ikehara (With 2 Figures)	252
Dynamics of Free and Momentarily Localized Excitons in HgI ₂ and PbI ₂ . By J. Takeda, T. Goto, and M. Matsuoka (With 3 Figures) . .	256
Formation and Relaxation of Excitonic Magnetic Polarons in Cd _{1-x} Mn _x Te and Cd _{1-x} Mn _x Se By Y. Oka, I. Souma, and Y. Kashiwagi (With 3 Figures)	259
Space- and Time-Resolved Spectroscopy of the Ultrafast Exciton Motion at a Stacking Fault Interface in Layered BiI ₃ Crystals By T. Karasawa, T. Kawai, I. Akai, and Y. Kaifu (With 3 Figures)	262
Ultrafast Optical Dephasing of Two-Dimensional Excitons in BiI ₃ By A. Nakamura, Y. Ishida, T. Yajima, T. Karasawa, I. Akai, and Y. Kaifu (With 3 Figures)	266

Ultrafast Relaxation of Localized Excitations in Solids By Y. Kayanuma (With 4 Figures)	269
Double Laser Excitation Spectroscopy on Picosecond Photochemical Reactions in Alkali Halide Crystals By Y. Suzuki, H. Abe, and M. Hirai (With 3 Figures)	274
Femtosecond to Microsecond Dynamics of Photoexcitations in a Polydiacetylene Film By T. Kobayashi, M. Yoshizawa, K. Ichimura, and M. Taiji (With 3 Figures)	277
Ultrashort Surface-Plasmon and Phonon Dynamics By M. van Exter and A. Lagendijk (With 2 Figures)	280
Femtosecond Image-Potential Dynamics in Metals By R.W. Schoenlein, J.G. Fujimoto, G.L. Eesley, and W. Capehart (With 2 Figures)	283

**Part VI Dynamical Processes in Semiconductor Quantum Wells
 and Microstructures**

Femtosecond Luminescence Spectroscopy: Investigation of Semiconductors and Semiconductor Microstructures By J. Shah, T.C. Damen, and B. Deveaud (With 5 Figures)	288
Femtosecond Carrier-Carrier Scattering Dynamics in p-Type and n- Type Modulation-Doped Quantum Wells By W.H. Knox, D.S. Chemla, G. Livescu, J.E. Henry, J.E. Cunningham, and S.M. Goodnick (With 2 Figures)	294
Cooling of Hot Carriers in Three- and Two-Dimensional $\text{Ga}_{0.47}\text{In}_{0.53}\text{As}$ By H. Lobentanzer, W. Stolz, and K. Ploog (With 3 Figures)	297
Tunneling Processes in AlAs/GaAs Double Quantum Wells By T. Tada, A. Yamaguchi, T. Ninomiya, H. Uchiki, T. Kobayashi, and T. Yao (With 4 Figures)	300
Picosecond Laser Study of Electron Dynamics in Resonant Tunneling Structures By M. Tsuchiya, T. Matsusue, and H. Sakaki (With 3 Figures)	304
Phase Relaxation of Two-Dimensional Excitons in a GaAs Single Quantum Well By A. Honold, L. Schultheis, J. Kuhl, and C.W. Tu (With 1 Figure)	307

Intra-Well and Cross-Well Transport Measurements in Multiple Quantum Wells Using Transient Gratings By R.J. Manning, A. Miller, D.W. Crust, D. Herbert, and K. Woodbridge (With 3 Figures)	311
Pulse Propagation in GaAs Quantum Wells By Y. Masumoto and M. Adachi (With 3 Figures)	315
Excitonic-Polariton Propagation in a GaAs/AlGaAs Quantum Well By K. Ogawa, T. Katsuyama, and H. Nakamura (With 2 Figures) .	318
Investigation of Intersubband Relaxation in GaAs/Al _x Ga _{1-x} As Quantum Well Structures by an Infrared Bleaching Technique By A. Seilmeier, M. Wörner, H.-J. Hübner, G. Weimann, and W. Schlapp (With 2 Figures)	321
Time-Resolved Photoluminescence Spectroscopy of GaAs Quantum Wells with 1 W Picosecond Light Pulses Generated from a Visible Diode Laser By H. Yokoyama, M. Fujii, M. Sugimoto, H. Iwata, K. Onabe, and T. Suzuki (With 3 Figures)	324
Light-Induced Selection Rules in Semiconductors Using Ultrashort Pulses By M. Joffre, D. Hulin, A. Migus, A. Antonetti, and M. Combescot (With 2 Figures)	328
Simultaneous Virtual and Two-Photon Femtosecond Excitations in GaAs MQWS By W.H. Knox, J.B. Stark, D.S. Chemla, D.A.B. Miller, and S. Schmitt-Rink (With 3 Figures)	331
Ultrafast Control of Quantum Interference Currents by Virtual Charge Polarizations in Biased Quantum Well Structures By M. Yamanishi, M. Kurosaki, Y. Osaka, and S. Datta (With 2 Figures)	334
Ultrafast Inter-Subband Relaxation of Photoexcited Carriers in Semiconductor Quantum Dots By T. Takagahara	337
Ultrafast Optical Nonlinearity in Semiconductor-Doped Glasses Controlled Through the Trapping State By M. Tomita, T. Matsumoto, and M. Matsuoka (With 6 Figures) .	340

Part VII **Nonlinear Optics, Coherent Spectroscopy and Spectroscopic Methods**

Femtosecond Photon Echoes By C.V. Shank, P.C. Becker, H.L. Fragnito, and R.L. Fork (With 3 Figures)	344
Fourier-Transform Spectroscopy in Dye-Doped Polymer Films Using Femtosecond Accumulated Photon Echo By S. Saikan (With 3 Figures)	349
Ultrafast Dynamics of Excitons and Polarons in Molecular Aggregates By S. de Boer and D.A. Wiersma (With 2 Figures)	354
Femtosecond Relaxation Studies of Semiconductors and Large Molecules By C.L. Tang, F.W. Wise, I.A. Walmsley, D. Edelstein, and E. Wachman (With 3 Figures)	357
Coherent Time- and Frequency-Domain Spectroscopy with a Picosecond Distributed Feedback Dye Laser By G.M. Gale, P. Schanne, and P. Ranson (With 2 Figures)	363
Raman Quantum Beats Obtained by Impulsive Stimulated Raman Scattering Close to an Electronic Resonance By J. Chesnoy and A. Mokhtari (With 3 Figures)	366
Picosecond Pump-Probe Interferometry of Nonlinear-Refractive Materials By D. Cotter, C.N. Ironside, B.J. Ainslie, and H.P. Girdlestone (With 2 Figures)	369
Measurement of Ultrashort Phase Relaxation Time of Semiconductor- Doped Glasses with Chirped Pulses By T. Tokizaki, Y. Ishida, and T. Yajima (With 4 Figures)	372
Ultrafast Fluorometry Using Temporally Incoherent Light By S. Asaka and K. Watanabe (With 3 Figures)	375
Femtosecond Kerr Dynamics and Three-Beam Degenerate Four- Wave Mixing with Incoherent Light By T. Hattori, A. Terasaki, Xusan Cheng, and T. Kobayashi (With 1 Figure)	378
Fluorescence Lifetime Measurement by Optical Kerr Shutter Gated with Incoherent Light By H. Nakatsuka, Y. Katashima, K. Inouye, and R. Yano (With 3 Figures)	381

New Method for the Measurement of Dephasing Time Using Incoherent Light with Reduced Noise and Its Application to CdS Fine Particles. By K. Misawa, T. Hattori, Y. Ohashi, H. Itoh, and T. Kobayashi (With 4 Figures)	384
Estimation of Ultrafast Relaxation Parameters from Excitation Spectra for Second-Order Optical Processes By S. Kinoshita and T. Kushida	387
Rise-Fall Ambiguities and Their Removal from Frequency-Domain Ultrafast-Measurement Techniques. By R. Trebino, C.E. Barker, and A.G. Kostenbauder (With 2 Figures)	390
Time-Resolved Resonant Light Scattering of an Electron-Hole System in an Intense Laser Field By T. Iida and T. Higashimura (With 4 Figures)	393
Microscopic Theory of Ultrafast Nonlinear Optical Phenomena in an Electron-Phonon System By M. Hama, M. Aihara, and M. Yokota (With 2 Figures)	396
Weak Localization of Femtosecond Laser Pulses by Random Media By R. Vreeker, M.P. van Albada, R. Sprik, and A. Lagendijk (With 2 Figures)	399
Measurements of the Electronic Wave Function in the Time Domain By L.D. Noordam, A. ten Wolde, and H.B. van Linden van den Heuvell (With 1 Figure)	402
Above-Threshold Ionization Observed in the Femtosecond Regime By H.B. van Linden van den Heuvell, H.G. Muller, P. Agostini, G. Petite, A. Antonetti, M. Franco, and A. Migus (With 1 Figure)	404
Two-Photon Absorption Sampling Spectroscopy for Fast Transient Luminescence Measurements By Y. Takagi and K. Yoshihara (With 3 Figures)	407
Application of the Time Characteristics of Synchrotron Radiation to Transient Spectroscopy By T. Mitani, H. Okamoto, Y. Takagi, I. Yamazaki, M. Watanabe, K. Fukui, S. Koshihara, and C. Ito (With 4 Figures)	410

Part VIII Dynamics on Surfaces and at Interfaces

Femtosecond Laser Photoionization Mass Spectrometry of Molecules on Surfaces. By S.V. Chekalin, V.V. Golovlev, A.A. Kozlov, V.S. Letokhov, Y.A. Matveetz, and A.P. Yartsev (With 3 Figures)	414
---	-----

Picosecond Photoionization Mass Spectroscopy and Optical Spectroscopy of Hot Semiconductor Surfaces By D. von der Linde, B. Danielzik, K. Sokolowski-Tinten, and P. Harten (With 4 Figures)	420
Picosecond Surface Reaction Dynamics and Carrier Processes at Semiconductor Interfaces By R.J. Dwayne Miller, J.J. Kasinski, L.A. Gomez-Jahn, and L. Min (With 3 Figures)	424
Direct Observation of Photodynamics in Opaque Organic Microcrystals: A Picosecond Diffuse Reflectance Laser Photolysis Study By N. Ikeda, M. Koshioka, H. Masuhara, N. Nakashima, and K. Yoshihara (With 3 Figures)	428
Sequential Excitation Energy Transport in Stacking Multilayers: A Comparative Study Between Photosynthetic Antenna and Langmuir-Blodgett Multilayers By I. Yamazaki, N. Tamai, and T. Yamazaki (With 1 Figure)	431
Fluorescence Lifetime of Dye Molecules Near a Metal Surface By F.R. Aussenegg, A. Leitner, M.E. Lippitsch, and H. Reinisch (With 3 Figures)	434
Molecular Aspects of Fast Fluorescence Dynamics in Amorphous Poly(N-Vinylcarbazole) Films By H. Sakai, A. Itaya, and H. Masuhara (With 2 Figures)	437

Part IX Energy Transfer and Relaxation

Picosecond and Femtosecond Infrared Spectroscopy with CW Diode Lasers By P. Anfinrud, C. Han, P.A. Hansen, J.N. Moore, and R.M. Hochstrasser (With 4 Figures)	442
Vibrational Relaxation Measurements of Carbon Monoxide on Metal Clusters By E.J. Heilweil, R.R. Cavanagh, and J.C. Stephenson (With 1 Figure)	447
Vibrational Relaxation Pathways of the N-H Stretch of Pyrrole in Liquids By J.R. Ambroseo and R.M. Hochstrasser (With 2 Figures)	450
Picosecond Infrared Spectroscopy of Semiconductors and Molecules By W. Kaiser, R.J. Bäuerle, T. Elsaesser, H.-J. Hübner, and A. Seilmeier (With 4 Figures)	452

Time- and Frequency-Resolved Infrared Spectroscopy with Picosecond Pulses. By H. Graener, T.-Q. Ye, R. Dohlus, and A. Laubereau (With 2 Figures)	458
Femtosecond Dephasing Processes of Molecular Vibrations By W. Zinth, W. Holzapfel, and R. Leonhardt (With 3 Figures) . . .	461
Effects of Coherence Transfer on Time-Resolved Coherent Anti-Stokes Raman Scattering and Transient Response of Resonant Light Scattering from Molecules By M. Hayashi, Y. Nomura, Y. Fujimura, and Y. Ohtsuki (With 2 Figures)	464
Vibrational Dynamics in the S_1 and S_0 States of Dye Molecules, Studied Separately by Femtosecond Polarization Spectroscopy By G. Angel, R. Gagel, and A. Laubereau (With 2 Figures)	467
Femtosecond Time and Frequency Resolved Fluorescence Spectroscopy of a Dye Molecule By A. Mokhtari, J. Chesnoy, and A. Laubereau (With 3 Figures) . . .	470
Supercontinuum Spectroscopy of Ethyl Violet Using a Simple Pulse Compression Technique. By M.M. Martin, F. Nesa, E. Breheret, and Y.H. Meyer (With 6 Figures)	473
The Effect of Overlapping Electronic Excited States on the Subpicosecond Fluorescence Anisotropy Decay Behavior of Tryptophan in Water By A. Ruggiero, D. Todd, and G.R. Fleming (With 2 Figures)	477
External Magnetic Field Effect on the Fluorescence of CS_2 Excited to the V^1B_2 State By H. Abe, H. Hayashi, T. Imamura, and S. Nagakura (With 3 Figures)	480
Picosecond Pulse Laser Photoelectron Spectra of Some Molecular Excited States By K. Kimura, K. Sato, K. Okuyama, and M. Takahashi (With 3 Figures)	483
Simultaneous Analysis of the Fluorescence Decay Surface of Tryptophan as a Function of Temperature, pH, Quencher and Emission Wavelength By N. Boens, L.D. Janssens, and F.C. De Schryver	486
Picosecond Laser Photolysis of 1,8-Dibromoanthraquinone in Carbon Tetrachloride at Room Temperature By T. Nakayama, M. Ito, Y. Yuhara, K. Ushida, and K. Hamanoue (With 3 Figures)	489

Double- to Triple-Minima Change in the Adiabatic Potential Energy Curve and Exciton Relaxation Dynamics in α -Perylene Crystals By K. Mizuno, M. Furukawa, A. Matsui, N. Tamai, and I. Yamazaki (With 2 Figures)	492
Time-Resolved Exciton Self-Trapping in Pyrene Crystals By H. Port and R. Seyfang (With 3 Figures)	495

Part X Chemical Reaction and Solvation Dynamics

Femtosecond Spectroscopy of Transition States in Reactions By A.H. Zewail (With 6 Figures)	500
Phase-Coherent Molecular Dynamics and Phase-Coherent Chemistry: Observation and Manipulation of Elementary Molecular Motion and Chemical Change By A.G. Joly, S. Ruhman, B. Kohler, and K.A. Nelson (With 4 Figures)	506
Ultrafast Laser Spectroscopy of Transient Ion Pair States in Solution By N. Mataga, H. Miyasaka, T. Asahi, S. Ojima, and T. Okada (With 3 Figures)	511
Geminate Recombination in Excited State Proton Transfer Reactions: Picosecond Dynamics in Electrolyte Solutions By E. Pines, D. Huppert, and N. Agmon (With 2 Figures)	517
Barrierless Isomerization in Solution Studied by Pico- and Subpicosecond Spectroscopy. By U. Åberg, E. Åkesson, H. Bergström, T. Gillbro, and V. Sundström (With 2 Figures)	520
Freezing of an Isomerization Reaction at Phase Transition By J. Korppi-Tommola, A. Hakkarainen, T. Hukka, and J. Subbi (With 3 Figures)	523
Trapping and Solvation of Electrons in Aqueous Media By A. Migus, S. Pommeret, N. Yamada, A. Antonetti, and Y. Gauduel (With 2 Figures)	527
Dynamics of Polar Solvation By G.R. Fleming and M.P. Maroncelli (With 4 Figures)	532
Ultrafast Molecular Dynamics in Solvating Liquids By W.T. Lotshaw, D. McMorro, C. Kalpouzos, and G.A. Kenney- Wallace (With 5 Figures)	537
Unified Theory of Solvation Dynamics in Nonlinear Optical Processes and Electron Transfer By S. Mukamel and Yi Jing Yan (With 2 Figures)	542

Coherent Vibrational Motion in Liquids: The Inhomogeneously Broadened Distribution of Intermolecular Oscillators By D. McMorrow, W.T. Lotshaw, T.R. Dickson, and G.A. Kenney-Wallace (With 2 Figures)	545
Hydrodynamic and Molecular Contributions to Rotational Diffusion in Liquids By D. Ben-Amotz, T.W. Scott, and J.M. Drake (With 2 Figures) . .	548
Influence of Functional Groups and Solvent on the Photoisomerization of Stilbenes. By N.S. Park, N. Sivakumar, E.A. Hoburg, and D.H. Waldeck (With 4 Figures)	551
Dynamics of Intramolecular Electron Transfer in Viscous Polar Solvents. By T. Okada, K. Nakatani, M. Hagihara, and N. Mataga (With 2 Figures)	555
Picosecond Investigation of Photoinduced Intramolecular Charge Transfer and Solvent Cage Relaxation Processes: Laser Dye DCM By J.C. Mialocq and M. Meyer (With 3 Figures)	559
Picosecond Ultraviolet Multiphoton Ionization and Geminate Charge Recombination in Hydrocarbon Solvents By Y. Hirata and N. Mataga (With 3 Figures)	562
Picosecond Ketyl Radical Spectroscopy By N.A. Borisevich, N.A. Lysak, S.A. Tikhomirov, and G.B. Tolstorozhev (With 3 Figures)	565
Electron Transfer Rates in Covalently Linked Donor–Acceptor Systems. By S. Doraiswamy, G.B. Maiya, N. Periasamy, and B. Venkataraman (With 2 Figures)	568
Excitation Transfer and Photo-Induced Electron Transfer in Conformationally Restricted Porphyrin Systems By A. Osuka, K. Maruyama, I. Yamazaki, and N. Tamai (With 2 Figures)	571

Part XI Dynamics of Biological Processes

Ultrafast Spectroscopy of Biological Processes By J.W. Petrich, J.L. Martin, and J. Breton (With 5 Figures)	576
Femtosecond Excited-State Reaction Dynamics of Retinal-Containing Photosystems By W. Zinth, J. Dobler, K. Dressler, and W. Kaiser (With 2 Figures)	581

Direct Observation of the Femtosecond Excited-State cis–trans Isomerization in Bacteriorhodopsin By R.A. Mathies, W.T. Pollard, C.H. Brito Cruz, and C.V. Shank (With 2 Figures)	584
Polarized Pump-Probe Spectroscopy of Exciton Transport in Bacteriochlorophyll <i>a</i> -Protein from <i>Prosthecochloris aestuarii</i> By T.P. Causgrove, S. Yang, and W.S. Struve (With 2 Figures) . . .	590
Picosecond Excitation Transport in Photosynthesis: Factors for Optimization of Light Harvesting By A. Freiberg, T. Pullerits, and K. Timpmann (With 2 Figures) . .	593
Excitation Energy Annihilation in Aggregates of Chlorophyll <i>a/b</i> Complexes By T. Gillbro, Å. Sandström, M. Spangfort, R. van Grondelle, and V. Sundström (With 2 Figures)	596
Picosecond Studies of Dynamic Solvent Effects on a DNA Intercalator by a Synchroscan Streak Camera System By M. Ishikawa (With 3 Figures)	599
Picosecond Fluorescence and Absorbance Study of Charge Separation and Charge Stabilization Processes in Photosystem II Particles. By A.R. Holzwarth, G.H. Schatz, H. Brock, and C.G. Colombano (With 2 Figures)	602
Picosecond Absorption Spectra of a Reaction Center from a Novel Thermophilic Photosynthetic Bacterium <i>Chromatium tepidum</i> By T. Nozawa, M. Terauchi, T. Kobayashi, and M. Hatano (With 2 Figures)	606
Time-Resolved Fluorescence Spectra of D-Amino Acid Oxidase: A New Fluorescent Species of the Coenzyme By F. Tanaka, N. Tamai, and I. Yamazaki (With 2 Figures)	610
Index of Contributors	613

Femtosecond Dephasing Processes of Molecular Vibrations

W. Zinth, W. Holzapfel, and R. Leonhardt

Physik Department E11, Technische Universität München,
Arcisstraße 21, D-8000 München 2, Fed. Rep. of Germany

Dynamical and static interactions in molecular liquids may be deduced from Raman and infrared spectra. In a limited number of cases the shape of the spectral band is understood by a definite line-broadening mechanism. Many realistic liquids, on the other hand, show complicated structures with non-Lorentzian asymmetric and partially overlapping bands. In addition, the spectral bandwidth may be considerably broader than 10 cm^{-1} corresponding to molecular time constants of less than 1 ps. The high time resolution now available in femtosecond coherent anti-Stokes Raman spectroscopy [1-3] gives the possibility to study various line-broadening mechanisms on the time scale of the molecular interaction.

In the present experiments we applied a femtosecond laser system allowing tunable excitation of vibrational modes between 300 cm^{-1} and 3000 cm^{-1} . The laser pulses derived from a femtosecond unidirectional ring dye laser (pulse duration $t_p = 80 \text{ fs}$) serve as the exciting and probing laser pulses at frequencies $\omega_L/4$. A standard synchronized tunable picosecond dye laser supplies the Stokes pulses at ω_S . Coherently scattered anti-Stokes light at $\omega_{AS} = 2\omega_L - \omega_S$ is detected as a function of the time delay between probing and exciting pulses (of perpendicular polarization). The high time resolution of the experimental system is readily demonstrated in Fig.1 showing the coherent anti-Stokes signal obtained from the OD-stretching mode of liquid D_2O . The full circles are experimental data taken at a sample temperature of 65°C . These data points are close to the experimental response function determined

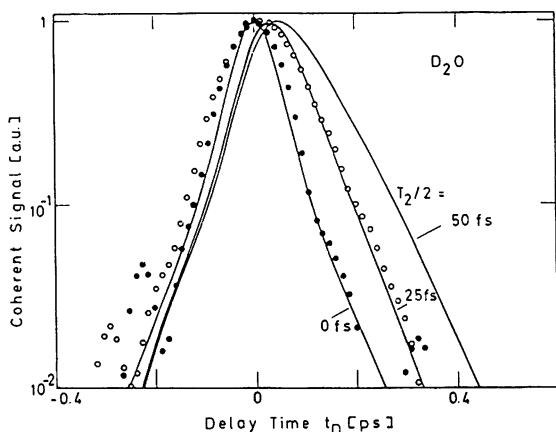


Fig. 1 Time-resolved coherent Raman signal from the OD vibration of liquid D_2O at 21°C (open circles) and 65°C (closed circles). The solid curves are calculated using a decay time $T_2/2$ of 0 fs, 25 fs, or 50 fs.

by a cross-correlation experiment. A different signal is obtained when the sample is held at a lower temperature of 21°C (open circles). Now the decay of the signal is delayed. The solid curves are calculated using the experimental response function and decay times of $T_2/2 = 0, 25$ fs, and 50 fs. We interpret the experimental data as follows: At low temperatures the coherent experiment studies the hydrogen bonded D_2O molecules. These complexes have a somewhat lower vibrational frequency than the non-bonded D_2O . We tentatively assign the dephasing time $T_2/2 = 25$ fs to these D_2O complexes. When the sample is heated the hydrogen-bonded complexes break up and the experiment probes the liquid of "monomeric" molecules. A very rapid decay of the signal is observed which is not resolved in our experiment.

Interesting information is obtained when studying the CH_3 -stretching modes of liquid methanol. The spontaneous Raman spectrum of methanol shows two strong bands at 2835 cm^{-1} and 2943 cm^{-1} . In addition there are large shoulders around the two major lines. Time-resolved coherent Raman scattering gives the result presented in Fig.2 (solid points). The signal exhibits a pronounced beating structure superimposed to an exponential decay. The solid curve of Fig.2 was calculated using homogeneous dephasing times for the two Raman-active modes. This curve fits the experimental points quite well. In order to take into account the possibility of inhomogeneous broadening, the calculation was repeated with an inhomogeneous contribution of 25% and 50% to the Raman linewidth (see broken curves of Fig.2). These curves noticeably deviate from the experimental data points. We conclude that the CH -stretching modes of methanol are predominantly homogeneously broadened.

Results on the molecular interactions are obtained when measuring the CH -stretching modes of liquid acetonitrile. In Fig.3a the coherent signal decay is shown over three orders of magnitudes. At later delay times the signal follows the exponential decay representing homogeneous dephasing with $T_2 = 1.74$ ps. At earlier delay times the experimental data deviate from the exponential slope. This fact is apparent from Fig.3b where the signal is multiplied by $\exp(2t_0/1.74\text{ps})$. An overshoot of the signal is seen at early delay times of up to 1.5 ps. Our first attempt was to fit the experimental decay curve by a Kubo line-shape model with an exponential decay of the frequency correlation function /5/. A ready agreement between theory and experiment was

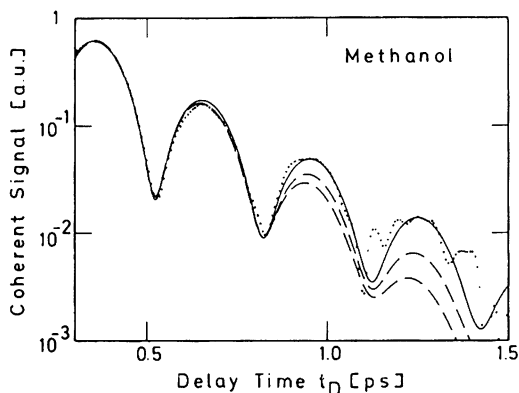


Fig. 2 Coherent signal of liquid methanol (points) and calculated curves assuming homogeneous dephasing (solid curve) and inhomogeneous line-broadening (broken curves) for 25% and 50% inhomogeneous contributions.

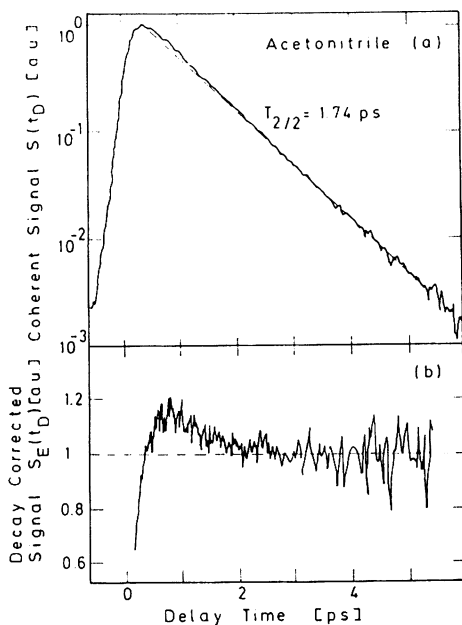


Fig. 3 Coherent signal from liquid acetonitrile. Intermolecular interactions show up by the overshoot of the signal at early delay times.

only obtained with a more elaborate theory, taking into account the close packing of the molecules in the liquid and the attractive part of the molecular interaction /6/.

Acknowledgement. The authors acknowledge valuable discussion with Professors W.Kaiser, S.F.Fischer, and E.W.Knapp.

References

- 1 R. Leonhardt, W. Holzapfel, W. Zinth, W. Kaiser: Chem. Phys. Lett. 133, 373 (1987)
- 2 R. Leonhardt, W. Holzapfel, W. Zinth, W. Kaiser, Rev. Phys. Appl. 22, 1735 (1987)
- 3 W. Zinth, R. Leonhardt, W. Holzapfel, W. Kaiser: IEEE J. Quant. Electron. QE-24, 455 (1988)
- 4 J. Döbler, H.H. Schultz, W. Zinth: Optics Commun. 57, 407 (1986)
- 5 D.W. Oxtoby, Adv. Chem. Phys. 40, 1 (1979)
- 6 E.W. Knapp, S.F. Fischer: J. Chem. Phys. 74, 89 (1981)